Article

Cite This: *Biomacromolecules* 2018, 19, 2870−2879

pubs.acs.org/Biomac

One Size Does Not Fit All: The Effect of Chain Length and Charge Density of Poly(ethylene imine) Based Copolymers on Delivery of pDNA, mRNA, and RepRNA Polyplexes

Anna K. Blakney,[†] Gokhan Yilmaz,[‡] Paul F. McKay,[†] C. Remzi Becer,*[,‡] and Robin J. Shattock*[,†]

[†]Department of Medicine, Division of Infectious Diseases, Section of Virology, Imperial College London, Norfolk Place, London W21PG, U.K.

[‡]Polymer Chemistry Laboratory, School of Engineering and Materials Science, Queen Mary University of London, London E1 4NS, U.K.

Supporting Information

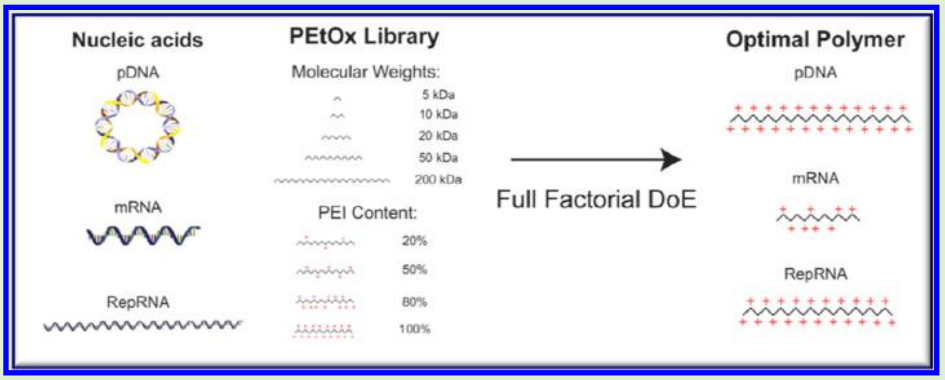

ABSTRACT: Nucleic acid delivery systems are commonly translated between different modalities, such as DNA and RNA of varying length and structure, despite physical differences in these molecules that yield disparate delivery efficiency with the same system. Here, we synthesized a library of poly(2-ethyl-2-oxazoline)/poly(ethylene imine) copolymers with varying molar mass and charge densities in order to probe how pDNA, mRNA, and RepRNA polyplex characteristics affect transfection efficiency. The library was utilized in a full factorial design of experiment (DoE) screening, with outputs of luciferase expression, particle size, surface charge, and particle concentration. The optimal copolymer molar mass and charge density was found as 83 kDa/100%, 72 kDa/100%, and 45 kDa/80% for pDNA, RepRNA, and mRNA, respectively. While 10 of the synthesized copolymers enhanced the transfection efficiency of pDNA and mRNA, only 2 copolymers enhanced RepRNA transfection efficiency, indicating a narrow and more stringent design space for RepRNA. These findings suggest that there is not a "one size fits all" polymer for different nucleic acid species.

INTRODUCTION

Nucleic acid delivery is becoming increasingly important in the context of vaccines and therapeutics as more platforms transition from academic concepts to clinical products.[1,2] A multitude of different nonviral delivery strategies have been used to deliver both DNA and RNA, including electroporation,[2,3] liposomes,[4] emulsions,[5] and polyplexes.[6−8] However, there are profound differences in the physical characteristics of DNA and RNA that contribute to disparate success with the same delivery system.[9−12] Plasmid DNA (pDNA) is double stranded and circular, and ranges in size from 2,000 to 10,000 base pairs. RNA is single stranded, except for some regions of double stranded secondary structure, and linear, and comes in a wider variety of sizes, from small interfering RNA (siRNA, 20−25 nt), to mRNA (mRNA, 2,000−5,000 nt) and self-amplifying replicon RNA (RepRNA, 8,000−12,000 nt).

Despite these differences, delivery strategies for new nucleic acid vaccines and therapies are usually evolved from historic formulations without taking the physical properties of novel nucleic acids into account. For example, replicon RNA has recently gained traction as an alternative to mRNA due to self-amplification properties, which typically yield higher protein expression for a similar dose of RNA.[5,13] However, delivery strategies for both mRNA and RepRNA to date are based on formulations that have been optimized for siRNA, despite vast differences in the size and structural components of these molecules.[5,14,15] Commercially available transfection reagents, such as Lipofectamine and PEI MAX, similarly discount the differences in nucleic acid species and generally recommend a fixed amount of transfection reagent per mass of nucleic acid or a constant ratio of the amine groups in the transfection reagent to phosphate in the nucleic acid (N/P ratio).[16−18] Kauffman et

Received: March 12, 2018
Revised: April 24, 2018
Published: April 26, 2018

DOI: 10.1021/acs.biomac.8b00429
Biomacromolecules 2018, 19, 2870−2879

Scheme 1. (a) Cationic Ring-Opening Polymerization of EtOx and Partial or Full Hydrolysis in Aqueous HCl and (b) Full Factorial Design of Experiment Parameters

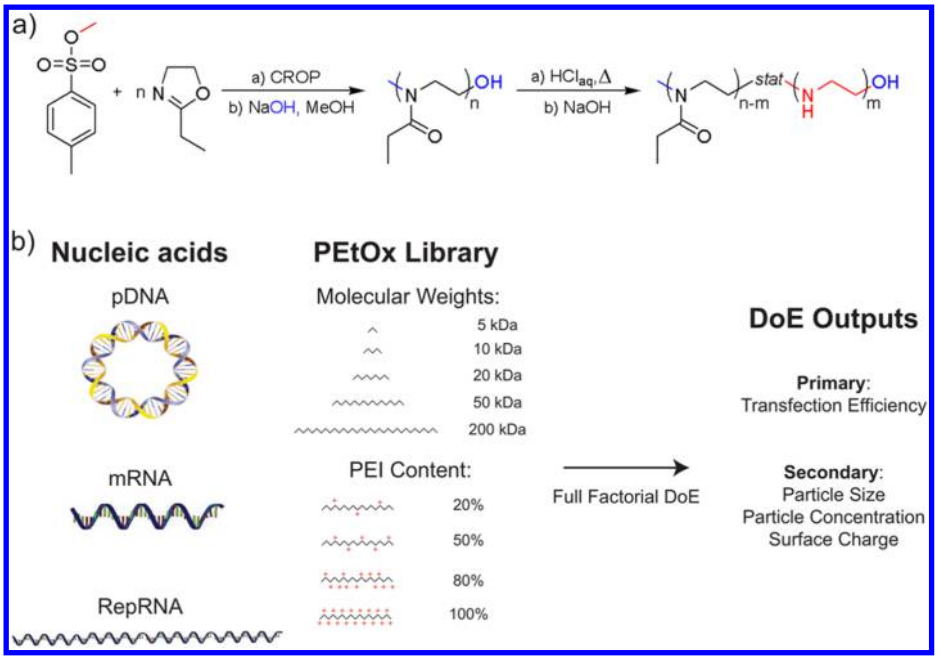

al. observed that optimization of liposomal formulation of mRNA by varying lipid ratios and structure increased the potency 7-fold but did not improve siRNA delivery, indicating that the design spaces for siRNA and mRNA are unique.[19] These examples question the common assumption that each platform works similarly well for each nucleic acid species, despite differences in their physical properties.

We hypothesized that the optimal cationic carrier characteristics and resulting complexation is unique to each nucleic species, even for molecules relatively similar in size and charge such as pDNA, mRNA, and RepRNA. To probe this hypothesis, we utilized copolymers of two widely studied linear polymers; poly(ethylene imine) (P(EI)) and poly(2-ethyl-2-oxazoline) (P(EtOx)) (Scheme 1).[6,20−24] These polymers have a positively charged secondary amine group that interacts with the negatively charged phosphate backbone of DNA or RNA to create a complex that facilitates uptake of the nucleic acid into cells.[25] These copolymers are particularly useful as it is possible to synthesize a wide variety of molecular weights, and the charge density of the polymer can be manipulated in a controlled manner using an acid hydrolysis reaction with well-known hydrolysis kinetics.[26,27] Previous studies have probed the effect of charge density and molecular weight on DNA transfection, but a systematic study comparing differences between DNA and RNA has not been performed.[21,23,28]

Given these dimensions, we sought to optimize the charge density and molar mass of a P(EtOx)-P(EI) copolymer for the formation of pDNA, mRNA, and RepRNA polyplexes. The pDNA, mRNA, and RepRNA all encoded firefly luciferase (fLuc) as a reporter protein and are 7,000 bp, 2,000 nt, and 9,500 nt in size, respectively. We designed and synthesized a library of P(EtOx)-P(EI) copolymers with molar mass ranging from 5 to 200 kDa with a variety of charge densities, represented by 20−100% hydrolysis. We utilized a full factorial design of experiments (DoE) approach to optimize the copolymers for each nucleic acid, with inputs of nucleic acid, molar mass, and charge density and outputs of luciferase expression and particle size, charge, and concentration. After DoE analysis, we used a Fit Model to predict the optimal polymer characteristics for each nucleic acid. Here, we show that varying the charge density and molar mass of the P(EtOx)-P(EI) copolymer differentially impacts the transfection efficiency and physical properties of each of the nucleic acid complexes. Furthermore, the theoretical optimal polymer varied for all three nucleic acid species, thus negating the common assumption of a "one size fits all" nucleic acid delivery vehicle.

EXPERIMENTAL SECTION

Materials. 2-Ethyl-2-oxazoline (EtOx, ≥ 99%), methyl *p*-toluenesulfonate (MeOTs, *98%*), and poly(2-ethyl-2-oxazoline) (**P4**, M_w = 50 000 g/mol and PDI = 3−4; and **P5**, M_w = 200 000 g/mol and PDI = 3−4) were purchased from Sigma-Aldrich Chemical Co. (Dorset, UK). EtOx and MeOTs were distilled and stored over activated 4 Å molecular sieves under an argon atmosphere. All other reagents and solvents were obtained at the highest purity available from Sigma-Aldrich Chemical Co. (Dorset, UK) and used as received unless stated otherwise. The dialysis tube (1 kDa MWCO) was purchased from Spectrum Laboratories (California, USA).

Instrument and Analysis. Proton nuclear magnetic resonance (^{1}H NMR) spectroscopy (Bruker DPX-400/600) was used to determine the chemical structure of the synthesized polymers. Samples were dissolved at 5 mg mL^{-1} concentration in D_2O or CD_3OD solvents depending on the solubility of the samples. Size-exclusion chromatography (SEC) measurements were conducted on an Agilent 1260 infinity system operating in DMF with 5.0 mM NH_4BF_4 and equipped with a refractive index detector (RID) and variable wavelength detector (VWD), 2 PLgel 5 μm mixed-C columns (300 × 7.5 mm), a PLgel 5 mm guard column (50 × 7.5 mm), and an autosampler. The instrument was calibrated with linear poly(methyl methacrylate) standards in a range of 550 to 46890 g/mol.

Methods. *Microwave-Assisted Homopolymerization of EtOx.* As a general procedure, a polymerization solution was prepared by the addition of initiator (methyl *p*-toluenesulfonate), monomer (EtOx), and solvent (acetonitrile) under inert atmosphere. The total monomer concentration was adjusted to 4 M with a monomer to initiator ratio of [EtOx]/[I] = 50:1, 100:1, and 200:1 for each polymer. Microwave vials were preheated to 150 °C and were allowed to cool to room

DOI: 10.1021/acs.biomac.8b00429
Biomacromolecules 2018, 19, 2870−2879

temperature under an argon atmosphere before the polymerization solutions were transferred into vials. The heating/cooling cycle is performed to ensure the dryness of the vials. Vials were capped, and the solutions were allowed to polymerize at 140 °C for 15, 20, and 30 min in the microwave synthesizer, respectively. After cooling, the reaction was quenched by the addition of 25 μL of MeOH. Samples were taken for ^{1}H NMR and SEC analysis to determine the monomer conversion and the molar mass and dispersity ($Đ$) of the polymers. The obtained copolymers were purified by precipitation in ice-cold diethyl ether twice and then dried in a vacuum oven at 40 °C for 3 h.

P(EtOx)$_m$: ^{1}H NMR (CD_3OD, 298 K, 400 MHz) δ = 3.82−3.26 (4 H, $-CH_2-CH_2-N-$), 2.42−2.14 (2H, $-NCOCH_2-CH_3$), 1.18−0.98 (3H, $-NCOCH_2-CH_3$) ppm.

Partial and Full Hydrolysis of P(EtOx)s. To obtain a specific degree of hydrolysis of the poly(EtOx)s, the kinetic study of **P2** was carried out according to a literature procedure.[27] A stock solution of each polymer (amide concentration = [A] = 0.48M) with a concentration of 1 M $HCl_{(aq)}$ was heated for different periods at 120 °C according to the kinetic study in a microwave synthesizer. The linear poly(ethylenimine)s (P(EI)s) with different Degrees of Polymerisation (DP) were produced by fully hydrolyzed P(EtOx)s in the presence of 3 M $HCl_{(aq)}$ solution for different periods at 180 °C. After the polymerization reactors were cooled down by compressed air, they were neutralized with 4 M $NaOH_{(aq)}$ solution. Samples were taken to measure ^{1}H NMR to determine the conversion of P(EtOx) to P(EI) using the signals of the hydrolysis products. Subsequently, the mixture was directly transferred to one dialysis tubing and dialyzed against water for 3 days after which the hydrolyzed polymers could be recovered by freeze-drying.

P((EtOx)$_{m\text{-}n}$-*co*-(EI)$_n$): ^{1}H NMR (CD_3OD, 298 K, 400 MHz): δ = 3.82−3.26 (4 H, $-CH_2-CH_2-N$-), 3.06−2.62 (4H, -NH$-CH_2-CH_2-$), 2.42−2.14 (2H, $-NCOCH_2-CH_3$), 2.18−2.00 (CH_3CH_2COOH), 1.24−0.82 (3H, $-NCOCH_2CH_3$, 3H, CH_3CH_2COOH) ppm.

P(EI)$_m$: ^{1}H NMR (CD_3OD, 298 K, 400 MHz): δ = 2.98−2.54 (4H, -NH$-CH_2-CH_2-$) ppm.

Plasmid DNA Synthesis and Purification. Mammalian codon optimized firefly luciferase was synthesized by GeneArt (Invitrogen, UK) and cloned into pcDNA3.1 (Invitrogen, UK). pDNA was transformed into *Escherichia coli*, grown in 50 mL cultures in LB with 1 mg mL^{-1} carbenicillin (SigmaAldrich, UK) and isolated and purified using a Plasmid Plus Maxiprep kit (QIAGEN, UK). pDNA concentration and purity were measured on a NanoDrop One (ThermoFisher, UK) prior to complexation.

RNA in Vitro Transcription and Purification. For the mRNA construct, the fLuc pcDNA3.1 pDNA was linearized using the NdeI and NotI restriction sites for 2 h at 37 °C, and then the enzymes were heat-inactivated at 65 °C for 20 min. For the replicon RNA construct, the fLuc gene was cloned into a plasmid encoding the nonstructural proteins of the Venezuelan equine encephalitis virus (VEEV) immediately after the subgenomic promotor using the restriction sites NdeI and MluI. The sequence was confirmed using Sanger sequencing (GATC Biotech, Germany). The pDNA was prepared as stated above and linearized using MluI for 2 h at 37 °C, and then the enzymes were heat-inactivated at 80 °C for 20 min. Capped in vitro transcripts were synthesized by adding 1 μg of linearized DNA to an mMessage mMachine reaction (Promega, UK) with an addition of 1 μL of GTP for the replicon RNA in each reaction to increase yield, and incubated for 2 h at 37 °C. RNA was then purified using MEGAclear Transcription Clean-Up Kit (Thermo, UK) according to the manufacturer's protocol. RNA concentration and purity were measured on NanoDrop One prior to complexation.

Nucleic Acid Complexation. Stock solutions of P(EtOx)-P(EI) copolymers were prepared at a concentration of 2 mg mL^{-1} in ultrapure H_2O and filtered using a 0.22 μm syringe filter (Millipore, Sigma, UK). Nucleic acid complexes were prepared by diluting the polymer and DNA/RNA into equal volumes of Dulbecco's modified Eagle's medium (DMEM) (Gibco, ThermoFisher, UK) with 0.5 mg mL^{-1} L-glutamine, adding the polymer solution to the RNA solution using a pipet, and immediately vortexing for 30 s. Because the P(EtOx)-P(EI) library consists of polymers with varying molar mass and charge density, the amount of polymer was normalized by keeping the molar amount of P(EI) (charged units) constant at 0.227 mmol and was calculated using the following equation:

$$\frac{\text{mol PEI}}{\text{L}} = \frac{\text{conc PEtOx}\left(\frac{\text{mg}}{\text{mL}}\right)\cdot M_{n,\text{Theo}}\left(\frac{\text{mol}}{\text{g}}\right)}{\frac{\%\ \text{PEI}}{100}}$$

The molar ratio of polymer to nucleic acid was fixed at 7000. Complexes were prepared fresh for transfection and stored at 4 °C until further analysis.

Transfection and Luciferase Assay. HEK 293T.17 cells (ATCC, USA) were plated at a density of 50,000 cells well^{-1} 48 h prior to transfection. The nucleic acid complexes were added to each well in a total volume of 100 μL and a total dose of 100 ng of DNA, mRNA, or RepRNA. Cells were exposed to complexes for 4 h, and then, the media was replaced with 100 μL of complete DMEM (10% fetal bovine serum, 5 mg mL^{-1} L-glutamine, and 5 mg mL^{-1} penicillin−streptomycin (ThermoFisher, UK)). After 24 h from the time of initial transfection, 50 μL of medium was removed from each well, 50 μL of ONE-Glo luciferase substrate (Promega, UK) was added, and the total 100 μL was transferred to a white 96-well plate and analyzed on a FLUOstar Omega plate reader (BMG LABTECH, UK) with a gain of 2000, 4000, and 3000 for DNA, mRNA, and RepRNA, respectively. MTS assay was performed on identical transfection reactions using a CellTiter 96 Aqueous One Solution Assay (Promega, UK) according to the manufacturer's protocol.

Characterization of Particle Size and Concentration. 100 μL of nucleic acid complexes were diluted into 900 μL of PBS (Sigma, UK) and equilibrated to room temperature prior to analysis. The particle size and concentration were analyzed on NanoSight LM10 (Malvern Instruments, UK) with NanoSight NTA 3.0 software (Malvern Instruments, UK) using an infusion rate of 20, capture duration of 1 min, gain of 2, and camera level of 7. Processing parameters were kept constant for all samples.

Characterization of Particle Charge. Samples were prepared identically to particle size and concentration characterization above and analyzed on a Zetasizer Nano ZS (Malvern Instruments, UK) with Zetasizer 7.1 software (Malvern Instruments, UK) using 730 μL of sample in a clear disposable 1 mL cuvette and the following settings: material refractive index of 1.529 and absorbance of 0.010 and dispersant viscosity of 0.8820 cP, refractive index of 1.330, and dielectric constant of 79. Each sample was analyzed for up to 100 runs until measurement equilibrated.

Design of Experiment and Statistical Analysis. DoE analysis was carried out in JMP, version 13.0 using a full factorial design with polymer molecular weight (MW), % P(EI), and nucleic acid as factors and particle mode size, concentration, surface charge, and luciferase expression as responses. The data were analyzed using a fit model of standard least squares for effect screening with the model effects designated as polymer MW, % P(EI), and the polymer MW*% P(EI) interaction. For analysis of each individual nucleic acid (e.g., DNA), the two extraneous nucleic acids (e.g., mRNA and RepRNA) were excluded from the model to examine the effects on each nucleic acid individually. The model for each nucleic acid was then used to predict the "optimal" P(EtOx)-P(EI) copolymer using polymer MW and % P(EI) as inputs and luciferase expression as the primary response. Graphs were prepared in GraphPad Prism, version 7.0.

RESULTS

Microwave-Assisted Homopolymerization of EtOx. Cationic ring opening polymerization (CROP) provides sufficient control for the living polymerization of 2-oxazoline monomers.[29−31] 2-Substituted-2-oxazolines are the most commonly used monomers for CROP, and they are promising candidates for biological applications due to their biocompatibility and low cytotoxicity.[32,33] Particularly, p(EtOx) is water-soluble and can also show a lower critical solution temperature

DOI: 10.1021/acs.biomac.8b00429
Biomacromolecules 2018, 19, 2870−2879

(LCST) behavior at specific chain length and concentration.[22] The polymerization of EtOx with different DPs (**P1**, **P2**, and **P3**) proceeded via CROP with a good control based on a protocol from previous studies.[34,35] Quantitative monomer conversion was obtained according to ^{1}H NMR spectra for each polymer (Table 1). As depicted in Figure 1a, all synthesized polymers (**P1**−**P3**) have a monomodal distribution with a low dispersity in the SEC, and the calculated molar mass values are in good agreement with the targeted molar mass values. However, **P4** and **P5** (M_w = 50,000 and M_w = 200,000 with PDI = 3−4, respectively) were purchased from Sigma-Aldrich and used to prepare high molecular weight P(EtOx)-P(EI) copolymers. It should be noted that these two commercial P(EtOx) polymers have a dispersity of 3−4 according to the supplier. However, in our SEC systems both have a bimodal distribution, and the dispersity values were calculated as 22 and 35. This unrealistic dispersity also indicates the inhomogeneous nature of the polymers. On the basis of these measurements, the number-average molar mass of **P4** and **P5** was calculated as 11200 and 23900 g/mol, respectively. Therefore, it should be noted that although **P1** with **P4** and **P3** with **P5** have very similar $M_{n,\,SEC}$ values, **P4** and **P5** contain a significant amount of high molar mass chains as well.

Table 1. Summary of Monomer Conversions, Number Average Molar Masses (M_n), and Molar Mass Distributions ($Đ$) of Cationic Ring Opening Polymerization of EtOx and Commercial P(EtOx)s

code	polymer	conversion[a] (%)	$M_{n,Theo}$[b] (g/mol)	$M_{n,SEC}$[c] (g/mol)	$Đ$
P1	$P(EtOx)_{50}$	99	4990	12200	1.19
P2	$P(EtOx)_{100}$	99	9950	17100	1.21
P3	$P(EtOx)_{200}$	99	19680	23800	1.24
P4	$P(EtOx)_{\sim 500}$		50000	11200	22
P5	$P(EtOx)_{\sim 2000}$		200000	23900	35

[a]Conversion (ρ) obtained from ^{1}H NMR. [b]$M_{n,\,Theo}$ = ($[M]_o$/$[MeOTs]_o$ × conversion × M_{mon}. [c]Determined by DMF SEC, relative to the PMM standard.

Partial and Full Hydrolysis of P(EtOx)s. P(EI)s in different structures have been widely used in gene delivery platforms due to their low cost, ease of preparation, long-term stability, and high loading capacity.[36,37] These positively charged polymeric nonviral gene carriers have an ability to create polyelectrolyte complexes (polyplexes) with negatively charged nucleic acids. In this work, the partial hydrolysis of P(EtOx)s was carried out under acidic conditions in 1 M HCl at 120 °C for different reaction times selected from the hydrolysis kinetic data (Table 2). P(EtOx)s were fully hydrolyzed in the presence of higher acid concentration (3 M HCl) and at higher temperature (180 °C) for different times to provide a full hydrolysis due to the slow progress of hydrolysis in the final stage. The conversion as a function of reaction time is slowing down due to the formation of EI units and the consequent decrease of free protons available to catalyze the hydrolysis. To prevent any degradation of the polymer backbone into oligomers, ^{1}H NMR was measured at 15 min

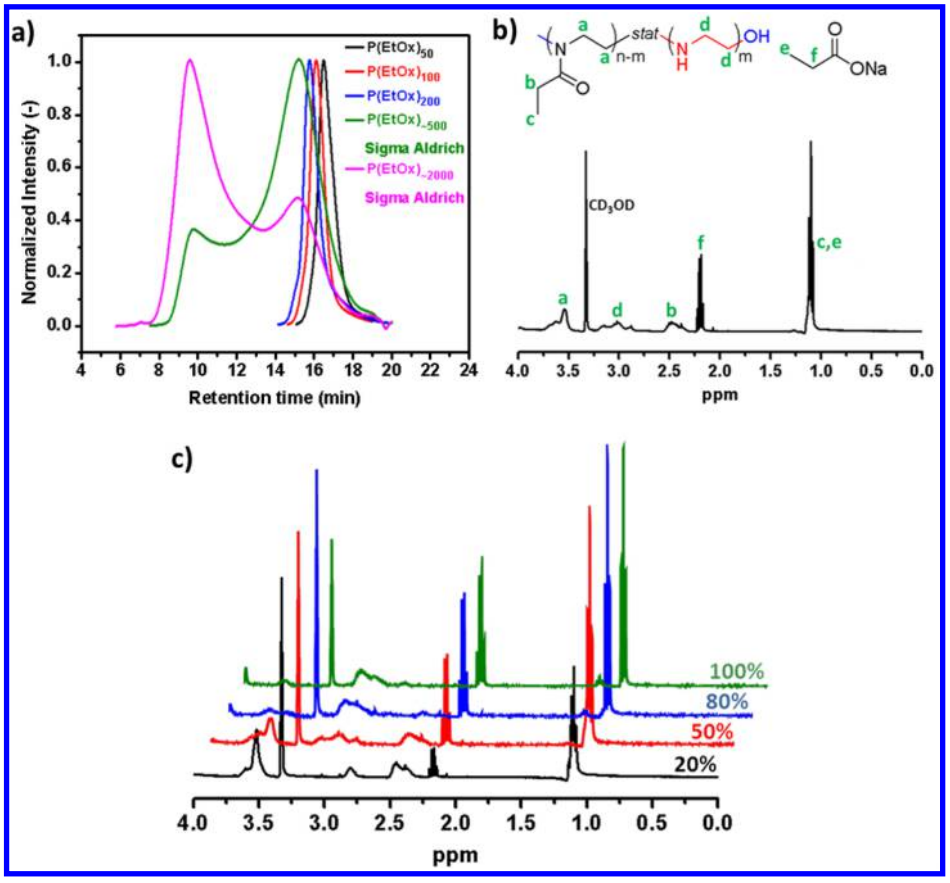

Figure 1. (a) SEC traces of the synthesized P(EtOx)s (**P1**−**P3**) and commercial P(EtOx)s (**P4**−**P5**). (b) ^{1}H NMR spectrum of 50% hydrolyzed **P2**, $P((EtOx)_{50}$-$(EI)_{50})$. (c) Series of ^{1}H NMR spectra in CD_3OD corresponding to different hydrolysis ratios of **P2**, $P(EtOx)_{100}$.

DOI: 10.1021/acs.biomac.8b00429
Biomacromolecules 2018, 19, 2870−2879

Table 2. Characteristics of P(EtOx)-P(EI) Copolymers Obtained by Acidic Hydrolysis of P(EtOx) Homopolymers with Different Degrees of Polymerization

code	polymer	DP[a]	% P(EI)[b]	$M_{n,Theo}$ (g/mol)
P1	$P(EI)_{50}$	50	100	2160
	$P((EtOx)_{10}\text{-}(EI)_{40})$	50	80	2715
	$P((EtOx)_{25}\text{-}(EI)_{25})$	50	50	3560
	$P((EtOx)_{40}\text{-}(EI)_{10})$	50	20	4395
P2	$P(EI)_{100}$	100	100	4320
	$P((EtOx)_{20}\text{-}(EI)_{80})$	100	80	5430
	$P((EtOx)_{50}\text{-}(EI)_{50})$	100	50	7120
	$P((EtOx)_{80}\text{-}(EI)_{20})$	100	20	8790
P3	$P(EI)_{200}$	200	100	8640
	$P((EtOx)_{40}\text{-}(EI)_{160})$	200	80	10860
	$P((EtOx)_{100}\text{-}(EI)_{100})$	200	50	14240
	$P((EtOx)_{160}\text{-}(EI)_{40})$	200	20	17580
P4	$P(EI)_{500}$	500	100	22280
	$P((EtOx)_{100}\text{-}(EI)_{400})$	500	80	27165
	$P((EtOx)_{250}\text{-}(EI)_{250})$	500	50	36140
	$P((EtOx)_{400}\text{-}(EI)_{100})$	500	20	43965
P5	$P(EI)_{2000}$	2000	100	89060
	$P((EtOx)_{400}\text{-}(EI)_{1600})$	2000	80	109750
	$P((EtOx)_{1000}\text{-}(EI)_{1000})$	2000	50	144530
	$P((EtOx)_{1600}\text{-}(EI)_{400})$	2000	20	177620

[a]On the basis of monomer feed and ^{1}H NMR. [b]On the basis of ^{1}H NMR.

intervals after 90% conversion of hydrolysis until all side chains of P(EtOx)s were cleaved to yield fully hydrolyzed P(EI)s. As seen in Figure 1c, the signals of P(EtOx) at 2.4 and 3.5 ppm decrease with increasing of ethylene imine units on the polymer backbone. Additionally, the signals of propionic acid sodium salt as a hydrolysis side product at 1.1 and 2.2 ppm increase with higher hydrolysis.

Increasing Charge Density, but Not MW, Enhances Transfection Efficiency. In order to investigate the impact of charge density and molecular weight of P(EtOx) polymers on the transfection efficiency of pDNA, mRNA, and RepRNA, we prepared complexes with each nucleic acid and P(EtOx) polymer in our library. The molar amount of P(EI) was kept constant at 2.27×10^{-4} mol no matter the molar mass or charge density of the polymer as the nucleic acid complexes only with the cationic amine groups. Luciferase expression was utilized as a proxy for transfection efficiency and expressed as RLU or fold change over the nucleic acid alone (Figure 2). Transfection efficiency of DNA had a trend of increasing with charge density and decreasing with polymer MW (Figure 2d), and polymers with MW greater than 20 kDa and above effectively increased the transfection efficiency up to 1000-fold compared to that of DNA alone (Figure 2a). mRNA was the only nucleic acid wherein the trend of increased transfection efficiency was significantly increased with higher charge density (Figure 2e, $p = 0.0341$) but was largely unaffected by polymer MW.

Polymers greater than 10 kDa were observed to enhance transfection efficiency of mRNA up to 80-fold compared to that of mRNA alone (Figure 2b). Similar to mRNA, there was a trend of increasing transfection efficiency of RepRNA with increasing charge density, but it was not statistically significant (Figure 2f). Only two polymers enhanced the transfection efficiency of RepRNA, including 50 kDa with 100% P(EI) and 200 kDa with 80% P(EI), which were 100- and 10-fold greater than RepRNA alone (Figure 2c). No cellular toxicity was observed at any of the polymer doses tested (Figure S2).

mRNA and DNA Particle Size Increases with Increasing Charge Density. After observing the effects of polymer charge density and MW on the transfection efficiency of DNA, mRNA, and RepRNA, we sought to characterize physical properties of the nucleic acid complexes in order to explain these differences. We observed how the average particle diameter of nucleic acid complexes is affected by the charge density and polymer MW (Figure 3).

DNA complexes ranged in diameter from 80 to 400 nm (Figure 3a), and increasing the % P(EI) significantly increased the average particle diameter (Figure 3d) ($p = 0.0040$). mRNA complexes similarly ranged in size from 80 to 450 nm (Figure 3b), and increasing the % P(EI) significantly increased the average particle size (Figure 3e). RepRNA complexes also ranged in size from 80 to 450 nm, although all but one sample was under 250 nm (Figure 3c). While there was a slight trend of increasing particle diameter with increasing % P(EI), it was not significant (Figure 3f). Polymer MW did not significantly affect any of the nucleic acid particle sizes, although the DNA complexes had a slight trend of increasing size with increasing MW (Figure 3d), while both RNA species were observed to have decreasing particle size with increasing MW (Figure 3e,f).

Charge Density and MW Disparately Affect DNA and RNA Complex Surface Charge. The physical properties of the nucleic acid complexes were further characterized by analyzing how the surface charge of the particles is impacted by changing the charge density and MW of the polymer (Figure 4). DNA, mRNA, and RepRNA are negatively charged, and neutralization of this charge in the presence of the cationic P(EtOx) polymers is an indicator of complexation. The surface charge of DNA complexes ranged from −7.0 mV to +1.5 mV (Figure 4a) and decreased with increasing charge density ($p = 0.0051$) but increased with increasing polymer MW ($p = 0.0011$) (Figure 4d). The mRNA complexes had a slightly narrower range of surface charge from −5.0 mV to +2.0 mV (Figure 4b). Unlike DNA, there was no impact of increasing the % P(EI), but increasing the polymer MW increased the surface charge (Figure 4e) ($p < 0.0001$). The RepRNA complexes ranged in surface charge from −7.0 mV to 2.0 mV (Figure 4c) and had similar trends as mRNA, but neither % P(EI) nor polymer MW significantly affected surface charge. Interestingly, for both DNA and RNA the only polymer that formed complexes with a positive surface charge was the 200 kDa with 100% P(EI). Despite individual differences among DNA, mRNA, and RepRNA, there was a general trend for each group of identical charge density (i.e., 50% P(EI)) where the 5 kDa was the most negative, while the 200 kDa was the most positive.

Increasing Charge Density Decreases Particle Concentration. While particle concentration is not a direct physical characterization of nucleic acid complexes, it can be an indicator of how efficiently molecules of the polymer are associating with DNA or RNA. Both DNA and RNA complexes ranged from 10^7–10^8 particles mL^{-1} (Figure 5). Increasing the % P(EI) exhibited a trend of decreased particle concentration for DNA (Figure 5a), while increasing the polymer MW significantly increased the particle concentration ($p = 0.0235$). Contrary to DNA, both RNA species were unaffected by polymer MW (Figure 5e,f), but increasing the charge density decreased the particle concentration, although this was significant for mRNA ($p = 0.0356$) but not RepRNA.

DOI: 10.1021/acs.biomac.8b00429
Biomacromolecules 2018, 19, 2870−2879

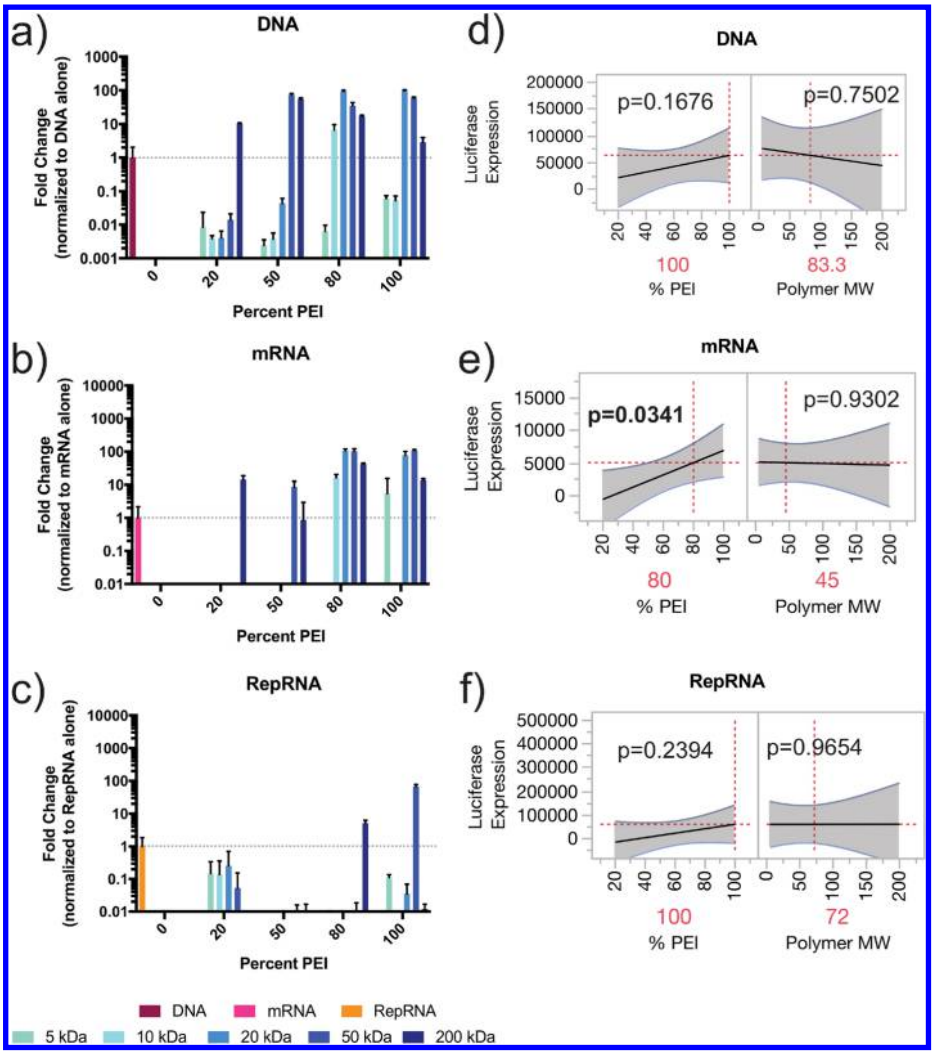

Figure 2. Luciferase expression in HEK 293T cells 24 h after transfection. (a–c) Fold change of luciferase expression measured in relative light units (RLU), normalized to the corresponding unformulated nucleic acid and calculated as the mean ± standard deviation for $n = 3$. (d–f) Prediction profiles based on DoE analysis for each nucleic acid with luciferase expression as the output. Gray shading indicates 95% confidence interval, and the p value in bold font indicates significance.

Optimal P(EtOx) Polymer Design for DNA, mRNA, and RepRNA. The functional and physical characterization of DNA and RNA complexes culminated in using the full factorial data to build a predictive model using a standard least-squares approach for effect screening. The model can then be used to identify which input factors should be considered and the relative importance of each of the inputs and their interactions. Polymer MW and % P(EI) were found to have statistically significant importance for DNA, mRNA, and RepRNA (Table 4). On the basis of log worth ranking, the polymer MW was the most important factor for all three nucleic acids. The interaction between polymer MW and % P(EI) (indicated as polymer MW*% P(EI)) was only statistically significant for mRNA but not DNA nor RepRNA.

The fit model was then used to design the optimal polymer for each nucleic acid (Table 3), with luciferase expression as the primary outcome, where the physical characterizations were secondary observational effects of this study. The optimal polymers for DNA, mRNA, and RepRNA are a MW of 83, 45, and 72 kDa and a % P(EI) of 100, 80 and 100, respectively.

DISCUSSION

This work identifies the optimal molecular weight and charge density of P(EtOx)-P(EI) copolymers for the in vitro delivery of pDNA, mRNA, and RepRNA. We show that polymers with the highest charge density, fully hydrolyzed P(EtOx)-P(EI) copolymers, increase the transfection efficiency for DNA and RepRNA but that a slightly lower charge density is optimal for mRNA transfection. DoE analysis revealed that the polymer molecular weight and charge density were significantly important for the fit models of DNA, mRNA, and RepRNA but that the interaction between these two inputs was significant only for mRNA. These data indicate that the physical properties of the delivery system, such as the available charge, charge density, and chain length, impact the complexation with DNA, mRNA, and RepRNA differently, which is likely due to variation in their physical properties. Within the burgeoning field of nucleic acid delivery, these findings emphasize that the optimal delivery platform characteristics do not directly translate between different nucleic acid species.

The optimal polymer for DNA was found to have a molecular weight of 83 kDa with 100% hydrolysis, which varies slightly from a previous report by Jeong et al. which found the

DOI: 10.1021/acs.biomac.8b00429
Biomacromolecules 2018, 19, 2870–2879

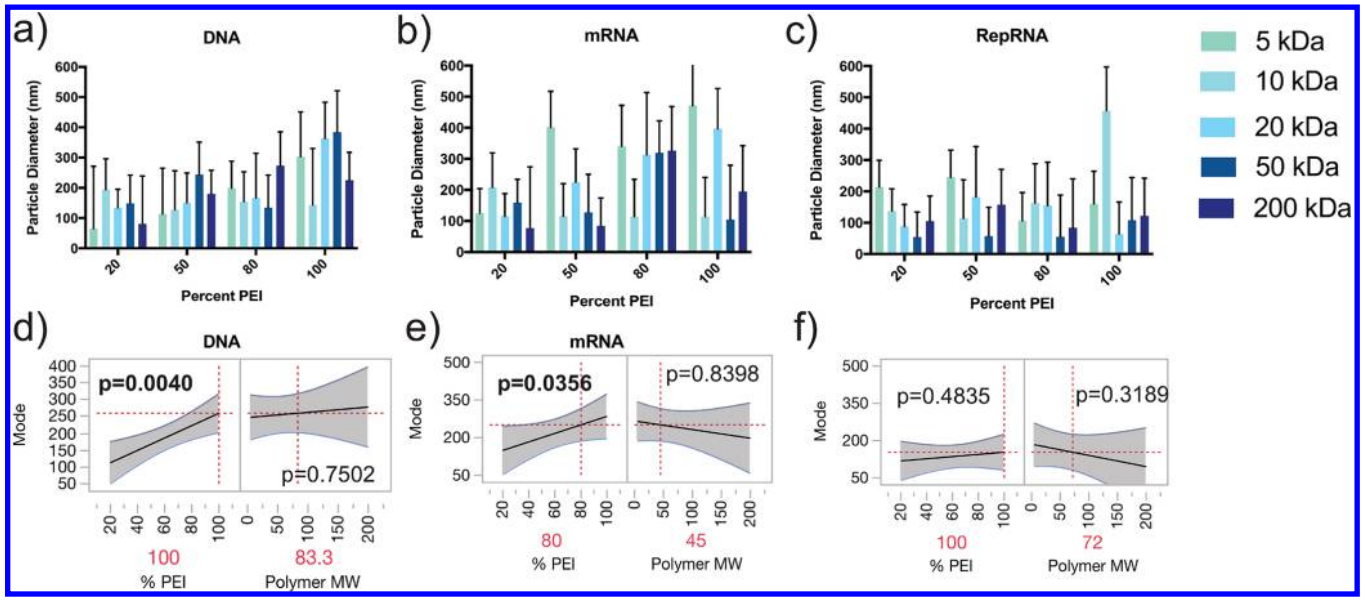

Figure 3. Particle sizes for nucleic acid/polymer complexes with varying P(EI) content, as measured by NanoSight Nanoparticle Tracking Analysis. (a–c) Measurements for DNA (a), mRNA (b), and RepRNA (c) expressed as mode ± standard deviation. (d–f) Prediction profiles based on DoE analysis for each nucleic acid with mode particle size as the output. Gray shading indicates 95% confidence interval, and the *p* value in bold font indicates significance.

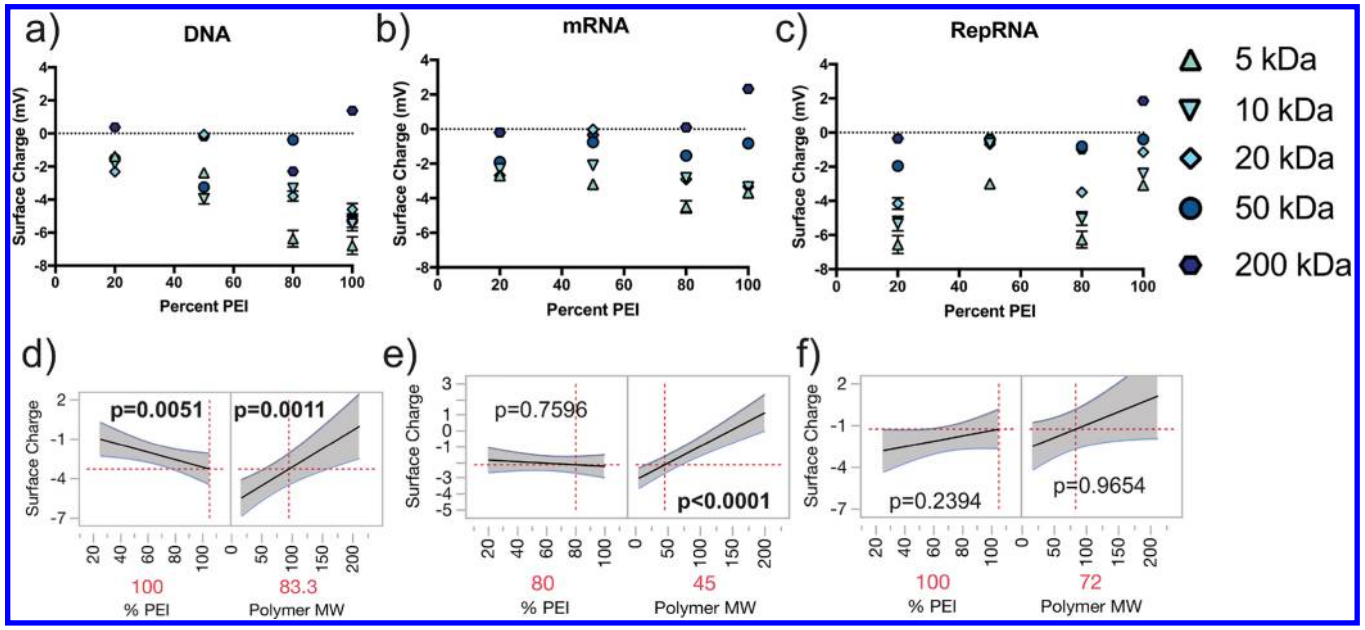

Figure 4. Surface charge of nucleic acid/polymer complexes as determined by Zetasizer. (a–c) Measurements for DNA (a), mRNA (b), and RepRNA (c) expressed as the mean ± standard deviation. (d–f) Prediction profiles based on DoE analysis for each nucleic acid with surface charge as the output. Gray shading indicates 95% confidence interval, and the *p* value in bold font indicates significance.

optimal polymer to be 50 kDa with 88% hydrolysis.[21] However, only four polymers were characterized in this study, with a MW of 50 or 200 kDa and varying hydrolysis from 52.6 to 91.6%, thus overlooking the full design space of P(EtOx)-P(EI) copolymers. The optimal polymer for RepRNA transfection efficiency was similar to that of DNA, with a molecular weight of 72 kDa and 100% hydrolysis. However, the optimal polymer for mRNA was found to be 80% hydrolysis, indicating that smaller RNA species may benefit from lower charge density. The smaller optimal molecular weight for mRNA, 45 kDa, also reflects the smaller size of mRNA compared to DNA and RepRNA. As the theoretical M_n values were used for the DoE analysis, the predicted polymers may not be completely accurate, but the general trends observed for PEI content and molecular content for DNA, mRNA, and RepRNA are informative. Because the transfection efficiency of DNA and RepRNA were maximized with the highest possible charge density, it is possible that using polymers with an even higher cationic charge, such as a quaternary amine, would be beneficial.[38,39] However, such a potent amine group may lead to irreversible binding of the nucleic acid and failure of endosomal escape from the complex.[40,41] In this case, it may be more suitable to design a highly charged ionizable polymer,

DOI: 10.1021/acs.biomac.8b00429
Biomacromolecules 2018, 19, 2870–2879

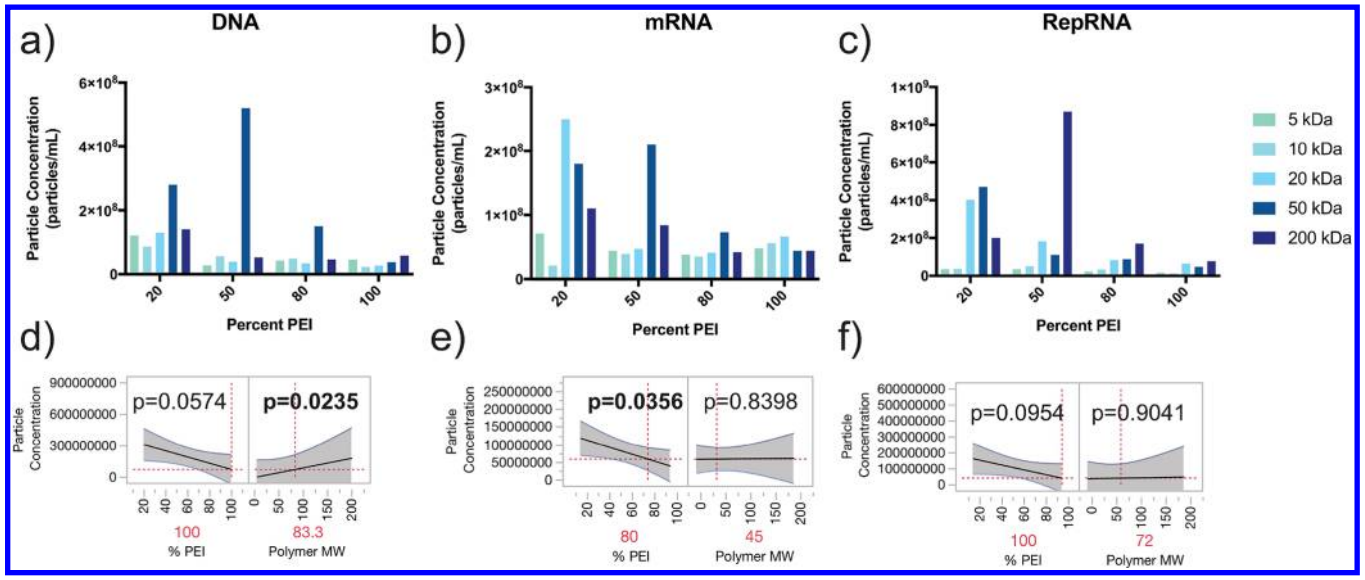

Figure 5. Particle concentration of nucleic acid/polymer complexes as determined by Nanosight. (a–c) Measurements for DNA (a), mRNA (b), and RepRNA (c) expressed as mean particle concentration. (d–f) Prediction profiles based on DoE analysis for each nucleic acid with surface charge as the output. Gray shading indicates 95% confidence interval, and the *p* value in bold font indicates significance.

Table 3. Summary of the Importance of DoE Input Factors for Each Nucleic Acid

nucleic acid	optimal % P(EI)	optimal polymer MW
DNA	100	83 kDa
mRNA	80	45 kDa
RepRNA	100	72 kDa

Table 4. DoE Optimized Parameters of P(EtOx) Polymer Design for Maximal Luciferase Expression

nucleic acid	DoE input factor	log worth	*p* value
DNA	polymer MW	2.960	0.00110
	% P(EI)	2.393	0.00404
	polymer MW* % P(EI)	1.028	0.09386
mRNA	polymer MW	4.687	0.00002
	% P(EI)	1.887	0.01296
	polymer MW* % P(EI)	1.477	0.03336
RepRNA	polymer MW	2.379	0.00418
	% P(EI)	1.690	0.02041
	polymer MW* % P(EI)	0.175	0.66666

similar to ionizable lipids that have been incorporated into liposomal delivery systems.[19,42,43]

The DoE analysis showed that increasing the % P(EI), but not molecular weight, positively correlated with enhanced transfection efficiency for each nucleic acid (Figure 2). Despite this trend, polymers with molecular weight ≥10 kDa showed enhanced transfection efficiency for DNA and mRNA, but only polymers with molecular weight ≥50 kDa showed any enhancement of transfection efficiency for RepRNA. This observation indicates that long, single stranded RNA species are more difficult to condense and deliver than similar sized DNA and shorter RNA species. The difficulty of condensation is reflected in the lack of a statistically significant correlation between increasing charge density and both particle size (Figure 3) and charge (Figure 4). While both DNA and mRNA showed increasing particle size with increasing charge density, and increasing surface charge with increasing polymer molecular weight, RepRNA was unaffected. On the basis of the decreasing particle concentration observed with increasing charge density for all three nucleic acid species (Figure 5), it appears that increasing the charge density universally increases the total number of nucleic acid molecules per polymer but not necessarily in a condensed state.

Despite the RepRNA being only twice the size of the mRNA, and similar in size to the DNA, only two of the P(EtOx)-P(EI) copolymers enhanced the transfection efficiency, whereas transfection efficiency was enhanced for DNA and mRNA by 10 of the copolymers. This emphasizes that RepRNA may be even more challenging to deliver than DNA and mRNA, with a stringently narrow design space; this observation is starting to be appreciated in the field of nucleic acid delivery.[44] We postulate that this is due to the long, single-stranded but highly structured nature of RepRNA; these molecules are physically larger and more highly charged than siRNA and mRNA and thus require innovative new delivery approaches. Further studies are required to provide insight into the structure, bioavailability, and endosomal escape kinetics of nucleic acid polyplexes and whether copolymeric delivery systems optimized in vitro are effective in vivo. Overall, this work shows that the physical differences in DNA, mRNA, and RepRNA impact how these nucleic acids interact with cationic P(EtOx)-P(EI) copolymers, resulting in a unique design space and optimal theoretical polymer for each.

CONCLUSION

In this work, we synthesized a library of P(EtOx)-P(EI) copolymers and optimized the molar mass and charge density for in vitro delivery of DNA, mRNA, and RepRNA using a DoE approach. The optimal charge density for DNA and RepRNA was found to be the fully hydrolyzed copolymer, while mRNA transfection efficiency peaked at 80% hydrolysis. Furthermore, the optimal molecular weight was 83 and 72 kDa for the larger nucleic acid species, DNA and RepRNA, respectively, while it was slightly lower, 45 kDa, for the smaller mRNA species. The DoE fit model elucidated that the design spaces for DNA and mRNA copolymers were more forgiving, while the RepRNA is more stringently narrow due to physical differences in length,

DOI: 10.1021/acs.biomac.8b00429
Biomacromolecules 2018, 19, 2870–2879

charge, and strand nature of the nucleic acids. These findings suggest that there is not a one size fits all polymer for nucleic acid delivery but rather that each nucleic acid species benefits from a tailored delivery system.

■ ASSOCIATED CONTENT

Supporting Information

The Supporting Information is available free of charge on the ACS Publications website at DOI: 10.1021/acs.biomac.8b00429.

Cytotoxicity of P(EtOx)-P(EI) in HEK cells, Luciferase Expression, Polymer Characterization via ^{1}H-NMR (PDF)

■ AUTHOR INFORMATION

Corresponding Authors

*(C.R.B.) E-mail: r.becer@qmul.ac.uk.

*(R.J.S.) E-mail: r.shattock@imperial.ac.uk.

ORCID

C. Remzi Becer: 0000-0003-0968-6662

Author Contributions

G.Y. performed the synthesis of the polymers. A.K.B. performed all complexation and cell work. All authors contributed to the design of the project and the writing of the manuscript.

Notes

The authors declare no competing financial interest.

■ ACKNOWLEDGMENTS

A.K.B. was funded by a Whitaker Foundation Post-Doctoral Fellowship, and G.Y. received funding from EPSRC (EP/P009018/1). R.J.S. and P.F.M. were funded by the EPSRC Future Vaccines Manufacturing Research Hub at Imperial College.

■ REFERENCES

(1) Pardi, N.; Hogan, M. J.; Porter, F. W.; Weissman, D. mRNA vaccines — a new era in vaccinology. *Nat. Rev. Drug Discovery* **2018**, *17*, 261.

(2) Lambricht, L.; Lopes, A.; Kos, S.; Sersa, G.; Préat, V.; Vandermeulen, G. Clinical potential of electroporation for gene therapy and DNA vaccine delivery. *Expert Opin. Drug Delivery* **2016**, *13* (2), 295−310.

(3) Johansson, D. X.; Ljungberg, K.; Kakoulidou, M.; Liljeström, P. Intradermal Electroporation of Naked Replicon RNA Elicits Strong Immune Responses. *PLoS One* **2012**, *7* (1), e29732.

(4) Ozpolat, B.; Sood, A. K.; Lopez-Berestein, G. Liposomal siRNA nanocarriers for cancer therapy. *Adv. Drug Delivery Rev.* **2014**, *66*, 110−116.

(5) Brito, L. A.; Chan, M.; Shaw, C. A.; Hekele, A.; Carsillo, T.; Schaefer, M.; Archer, J.; Seubert, A.; Otten, G. R.; Beard, C. W.; Dey, A. K.; Lilja, A.; Valiante, N. M.; Mason, P. W.; Mandl, C. W.; Barnett, S. W.; Dormitzer, P. R.; Ulmer, J. B.; Singh, M.; O'Hagan, D. T.; Geall, A. J. A Cationic Nanoemulsion for the Delivery of Next-generation RNA Vaccines. *Mol. Ther.* **2014**, *22* (12), 2118−2129.

(6) Taranejoo, S.; Liu, J.; Verma, P.; Hourigan, K. A review of the developments of characteristics of PEI derivatives for gene delivery applications. *J. Appl. Polym. Sci.* **2015**, *132* (25), 1−8.

(7) Debus, H.; Baumhof, P.; Probst, J.; Kissel, T. Delivery of messenger RNA using poly(ethylene imine)−poly(ethylene glycol)-copolymer blends for polyplex formation: Biophysical characterization and in vitro transfection properties. *J. Controlled Release* **2010**, *148* (3), 334−343.

(8) Kurtulus, I.; Yilmaz, G.; Ucuncu, M.; Emrullahoglu, M.; Becer, C. R.; Bulmus, V. A new proton sponge polymer synthesized by RAFT polymerization for intracellular delivery of biotherapeutics. *Polym. Chem.* **2014**, *5* (5), 1593−1604.

(9) Millar, D. P. Fluorescence studies of DNA and RNA structure and dynamics. *Curr. Opin. Struct. Biol.* **1996**, *6* (3), 322−326.

(10) Mao, S.; Sun, W.; Kissel, T. Chitosan-based formulations for delivery of DNA and siRNA. *Adv. Drug Delivery Rev.* **2010**, *62* (1), 12−27.

(11) Chien, P.-Y.; Wang, J.; Carbonaro, D.; Lei, S.; Miller, B.; Sheikh, S.; Ali, S. M.; Ahmad, M. U.; Ahmad, I. Novel cationic cardiolipin analogue-based liposome for efficient DNA and small interfering RNA delivery in vitro and in vivo. *Cancer Gene Ther.* **2005**, *12*, 321.

(12) Spagnou, S.; Miller, A. D.; Keller, M. Lipidic Carriers of siRNA: Differences in the Formulation, Cellular Uptake, and Delivery with Plasmid DNA. *Biochemistry* **2004**, *43* (42), 13348−13356.

(13) Brito, L. A.; Kommareddy, S.; Maione, D.; Uematsu, Y.; et al. Chapter Seven: Self-Amplifying mRNA Vaccines. *Nonviral Vectors for Gene Therapy: Physical Methods and Medical Translation*; Advances in Genetics; Elsevier, 2015; Vol. *89*, pp 179−233.

(14) Geall, A. J.; Verma, A.; Otten, G. R.; et al. Nonviral delivery of self-amplifying RNA vaccines. *Proc. Natl. Acad. Sci. U. S. A.* **2012**, *109*, 14604−9.

(15) Semple, S. C.; Akinc, A.; Chen, J.; Sandhu, A. P.; Mui, B. L.; Cho, C. K.; Sah, D. W. Y.; Stebbing, D.; Crosley, E. J.; Yaworski, E.; Hafez, I. M.; Dorkin, J. R.; Qin, J.; Lam, K.; Rajeev, K. G.; Wong, K. F.; Jeffs, L. B.; Nechev, L.; Eisenhardt, M. L.; Jayaraman, M.; Kazem, M.; Maier, M. A.; Srinivasulu, M.; Weinstein, M. J.; Chen, Q.; Alvarez, R.; Barros, S. A.; De, S.; Klimuk, S. K.; Borland, T.; Kosovrasti, V.; Cantley, W. L.; Tam, Y. K.; Manoharan, M.; Ciufolini, M. A.; Tracy, M. A.; de Fougerolles, A.; MacLachlan, I.; Cullis, P. R.; Madden, T. D.; Hope, M. J. Rational design of cationic lipids for siRNA delivery. *Nat. Biotechnol.* **2010**, *28*, 172.

(16) Dalby, B.; Cates, S.; Harris, A.; Ohki, E. C.; Tilkins, M. L.; Price, P. J.; Ciccarone, V. C. Advanced transfection with Lipofectamine 2000 reagent: primary neurons, siRNA, and high-throughput applications. *Methods* **2004**, *33* (2), 95−103.

(17) Delafosse, L.; Xu, P.; Durocher, Y. Comparative study of polyethylenimines for transient gene expression in mammalian HEK293 and CHO cells. *J. Biotechnol.* **2016**, *227*, 103−111.

(18) Mann, J. F. S.; McKay, P. F.; Arokiasamy, S.; Patel, R. K.; Klein, K.; Shattock, R. J. Pulmonary delivery of DNA vaccine constructs using deacylated PEI elicits immune responses and protects against viral challenge infection(). *J. Controlled Release* **2013**, *170* (3), 452−459.

(19) Kauffman, K. J.; Dorkin, J. R.; Yang, J. H.; Heartlein, M. W.; DeRosa, F.; Mir, F. F.; Fenton, O. S.; Anderson, D. G. Optimization of Lipid Nanoparticle Formulations for mRNA Delivery in Vivo with Fractional Factorial and Definitive Screening Designs. *Nano Lett.* **2015**, *15* (11), 7300−7306.

(20) Lambermont-Thijs, H. M. L.; Bonami, L.; Du Prez, F. E.; Hoogenboom, R. Linear poly(alkyl ethylene imine) with varying side chain length: synthesis and physical properties. *Polym. Chem.* **2010**, *1* (5), 747−754.

(21) Jeong, J. H.; Song, S. H.; Lim, D. W.; Lee, H.; Park, T. G. DNA transfection using linear poly(ethylenimine) prepared by controlled acid hydrolysis of poly(2-ethyl-2-oxazoline). *J. Controlled Release* **2001**, *73* (2), 391−399.

(22) Hoogenboom, R. Poly(2-oxazoline)s: A Polymer Class with Numerous Potential Applications. *Angew. Chem., Int. Ed.* **2009**, *48* (43), 7978−7994.

(23) Hsiue, G.-H.; Chiang, H.-Z.; Wang, C.-H.; Juang, T.-M. Nonviral Gene Carriers Based on Diblock Copolymers of Poly(2-ethyl-2-oxazoline) and Linear Polyethylenimine. *Bioconjugate Chem.* **2006**, *17* (3), 781−786.

(24) Becer, C. R.; Paulus, R. M.; Höppener, S.; Hoogenboom, R.; Fustin, C.-A.; Gohy, J.-F.; Schubert, U. S. Synthesis of Poly(2-ethyl-2-oxazoline)-b-poly(styrene) Copolymers via a Dual Initiator Route

Combining Cationic Ring-Opening Polymerization and Atom Transfer Radical Polymerization. *Macromolecules* **2008**, *41* (14), 5210−5215.
(25) Oh, Y. K.; Suh, D.; Kim, J. M.; Choi, H. G.; Shin, K.; Ko, J. J. Polyethylenimine-mediated cellular uptake, nucleus trafficking and expression of cytokine plasmid DNA. *Gene Ther.* **2002**, *9*, 1627.
(26) Van Kuringen, H. P. C.; Lenoir, J.; Adriaens, E.; Bender, J.; De Geest, B. G.; Hoogenboom, R. Partial Hydrolysis of Poly(2-ethyl-2-oxazoline) and Potential Implications for Biomedical Applications? *Macromol. Biosci.* **2012**, *12* (8), 1114−1123.
(27) de la Rosa, V. R.; Bauwens, E.; Monnery, B. D.; De Geest, B. G.; Hoogenboom, R. Fast and accurate partial hydrolysis of poly(2-ethyl-2-oxazoline) into tailored linear polyethylenimine copolymers. *Polym. Chem.* **2014**, *5* (17), 4957−4964.
(28) Mees, M.; Haladjova, E.; Momekova, D.; Momekov, G.; Shestakova, P. S.; Tsvetanov, C. B.; Hoogenboom, R.; Rangelov, S. Partially Hydrolyzed Poly(n-propyl-2-oxazoline): Synthesis, Aqueous Solution Properties, and Preparation of Gene Delivery Systems. *Biomacromolecules* **2016**, *17* (11), 3580−3590.
(29) Paulus, R. M.; Becer, C. R.; Hoogenboom, R.; Schubert, U. S. Acetyl halide initiator screening for the cationic ring-opening polymerization of 2-ethyl-2-oxazoline. *Macromol. Chem. Phys.* **2008**, *209* (8), 794−800.
(30) Krieg, A.; Weber, C.; Hoogenboom, R.; Becer, C. R.; Schubert, U. S. Block Copolymers of Poly(2-oxazoline)s and Poly(meth)-acrylates: A Crossover between Cationic Ring-Opening Polymerization (CROP) and Reversible Addition−Fragmentation Chain Transfer (RAFT). *ACS Macro Lett.* **2012**, *1* (6), 776−779.
(31) Weber, C.; Neuwirth, T.; Kempe, K.; Ozkahraman, B.; Tamahkar, E.; Mert, H.; Becer, C. R.; Schubert, U. S. 2-Isopropenyl-2-oxazoline: A Versatile Monomer for Functionalization of Polymers Obtained via RAFT. *Macromolecules* **2012**, *45* (1), 20−27.
(32) Weber, C.; Becer, C. R.; Guenther, W.; Hoogenboom, R.; Schubert, U. S. Dual Responsive Methacrylic Acid and Oligo(2-ethyl-2-oxazoline) Containing Graft Copolymers. *Macromolecules* **2010**, *43* (1), 160−167.
(33) Weber, C.; Becer, C. R.; Hoogenboom, R.; Schubertt, U. S. Lower Critical Solution Temperature Behavior of Comb and Graft Shaped Poly oligo(2-ethyl-2-oxazoline)methacrylate s. *Macromolecules* **2009**, *42* (8), 2965−2971.
(34) Wiesbrock, F.; Hoogenboom, R.; Leenen, M. A. M.; Meier, M. A. R.; Schubert, U. S. Investigation of the Living Cationic Ring-Opening Polymerization of 2-Methyl-, 2-Ethyl-, 2-Nonyl-, and 2-Phenyl-2-oxazoline in a Single-Mode Microwave Reactor. *Macromolecules* **2005**, *38* (12), 5025−5034.
(35) Wiesbrock, F.; Hoogenboom, R.; Leenen, M.; van Nispen, S. F. G. M.; van der Loop, M.; Abeln, C. H.; van den Berg, A. M. J.; Schubert, U. S. Microwave-Assisted Synthesis of a 42-Membered Library of Diblock Copoly(2-oxazoline)s and Chain-Extended Homo Poly(2-oxazoline)s and Their Thermal Characterization. *Macromolecules* **2005**, *38* (19), 7957−7966.
(36) Godbey, W. T.; Wu, K. K.; Mikos, A. G. Poly(ethylenimine) and its role in gene delivery. *J. Controlled Release* **1999**, *60* (2), 149−160.
(37) Lungwitz, U.; Breunig, M.; Blunk, T.; Göpferich, A. Polyethylenimine-based non-viral gene delivery systems. *Eur. J. Pharm. Biopharm.* **2005**, *60* (2), 247−266.
(38) Pack, D. W.; Hoffman, A. S.; Pun, S.; Stayton, P. S. Design and development of polymers for gene delivery. *Nat. Rev. Drug Discovery* **2005**, *4*, 581.
(39) Reineke, T. M.; Davis, M. E. Structural Effects of Carbohydrate-Containing Polycations on Gene Delivery. 2. Charge Center Type. *Bioconjugate Chem.* **2003**, *14* (1), 255−261.
(40) van de Wetering, P.; Moret, E. E.; Schuurmans-Nieuwenbroek, N. M. E.; van Steenbergen, M. J.; Hennink, W. E. Structure−Activity Relationships of Water-Soluble Cationic Methacrylate/Methacrylamide Polymers for Nonviral Gene Delivery. *Bioconjugate Chem.* **1999**, *10* (4), 589−597.
(41) Wolfert, M. A.; Dash, P. R.; Nazarova, O.; Oupicky, D.; Seymour, L. W.; Smart, S.; Strohalm, J.; Ulbrich, K. Polyelectrolyte Vectors for Gene Delivery: Influence of Cationic Polymer on Biophysical Properties of Complexes Formed with DNA. *Bioconjugate Chem.* **1999**, *10* (6), 993−1004.
(42) Liu, Y.; Huang, L. Designer Lipids Advance Systemic siRNA Delivery. *Mol. Ther.* **2010**, *18* (4), 669−670.
(43) Whitehead, K. A.; Dorkin, J. R.; Vegas, A. J.; Chang, P. H.; Veiseh, O.; Matthews, J.; Fenton, O. S.; Zhang, Y.; Olejnik, K. T.; Yesilyurt, V.; Chen, D.; Barros, S.; Klebanov, B.; Novobrantseva, T.; Langer, R.; Anderson, D. G. Degradable Lipid Nanoparticles with Predictable In Vivo siRNA Delivery Activity. *Nat. Commun.* **2014**, *5*, 4277−4277.
(44) Dowdy, S. F. Overcoming cellular barriers for RNA therapeutics. *Nat. Biotechnol.* **2017**, *35*, 222.

DOI: 10.1021/acs.biomac.8b00429
Biomacromolecules 2018, 19, 2870−2879